COR1-A Vacuum Calibration, July 2004

William Thompson
Clarence Korendyke
Eric Mentzell

July 29, 2004

We report here on the calibration and scattered light measurements of COR1-A, made in the NRL A13 vacuum tunnel, July 2004, prior to the formal delivery of the instrument to NRL. The primary purpose of this calibration activity was to test the scattered light properties, but it was also the first chance to test the instrument in vacuum, and with a cooled CCD. Using various configurations of the vacuum tank, the properties tested were scattered light, photometric calibration, resolution, and polarization.

1 Noise

Liquid nitrogen was used to cool the CCD detector down to temperatures close to that which it will see in flight. An LN_2 dewer inside the vacuum chamber was thermally coupled to the radiator mass mockup attached to the FPA. Temperature could be controlled either through heaters at the dewer end of the copper strap, or on the CCD itself. We were able to cool the CCD down below -50 C, but never managed to get down all the way to the -75 C expected in flight.

The effect of cooling the CCD is demonstrated in Figure 1. On the left is a dark image made when the CCD was relatively hot, at about +10 C, while the image on the right was taken when the CCD was much colder, at about -30 C. The images are not on the same scale—if they were, the cold case would appear mostly black. The exposure time was 10 seconds for both images.

By taking a series of exposure times at various CCD temperatures, one can separate out the dark current effects from readout noise. Figure 2 shows the average dark current in the CCD as a function of temperature.

There is a slight difference in thermal noise between images which use the shutter and those which don't. The reason has to do with overhead in the ITOS software associated with sending the commands for operating the shutter. The difference is approximately 0.75 seconds. Running the detector cold reduces the effect of this difference.

As well as thermal noise, the instrument is also subject to readout and pickup noise. Because the cabling between the FPA and the CEB was considerably longer than flight, there's more pickup noise than would be expected in flight, with an RMS of $\sim$9 DN.

2 Resolution

When the instrument resolution was tested with the Meade telescope system, an offset was applied to account for the difference between vacuum and the nitrogen purge at one atmosphere of pressure.

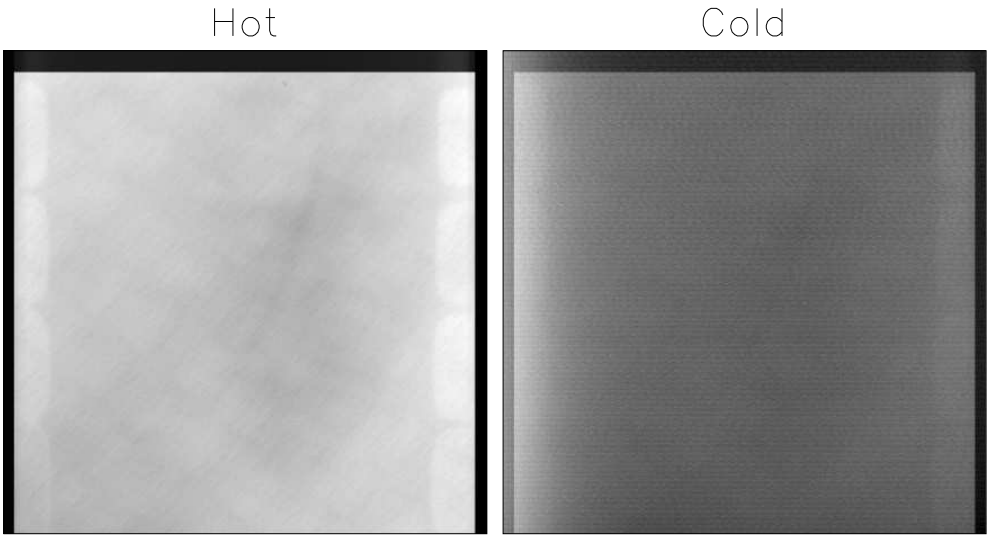

Figure 1: Dark images for "hot" (+10 C) and "cold" (-30 C) cases. Images are not on the same scale.

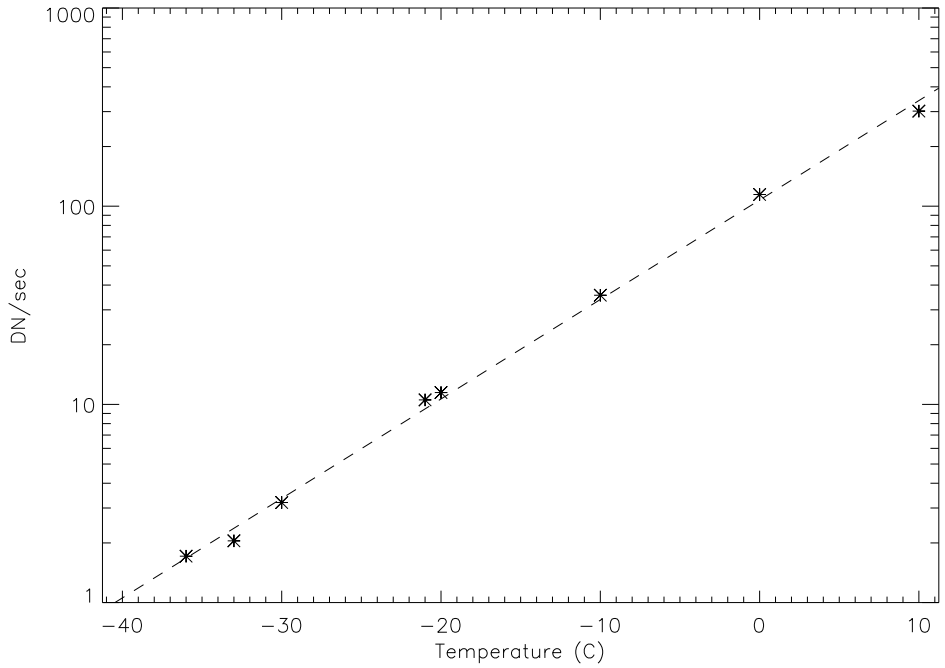

Figure 2: Average detector dark current as a function of CCD temperature.

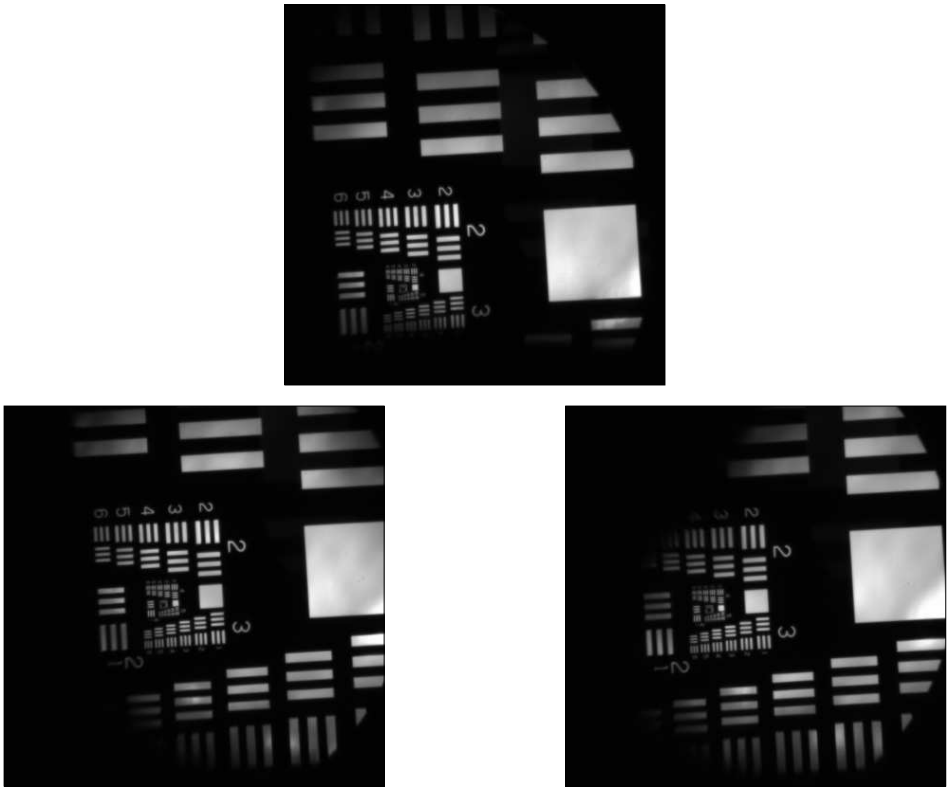

Figure 3: Air Force target images in vacuum.

The vacuum testing at NRL afforded an opportunity to test the on-orbit resolution without any need for corrections. The collimator at the end of the tank was focused to project an image of an Air Force 1951 resolution test target at infinity. The COR1-A instrument was then steered to place this image at various locations on the detector. The results are shown in Figure 3. Although the targets are slightly canted with respect to the detector pixels, a detailed examination of the images shows that the resolution extends down to the full-resolution Nyquist frequency (one line pair per 27 μm). These images were taken at a temperature of approximately -50 C.

When the resolution was tested during final assembly, the contrast was measured for group 4-1, whose bars were 1.5 full-resolution pixels wide. (When 2×2 binning is used, this would actually be above the Nyquist frequency.) Because the collimator used for the vacuum calibration has a slightly different magnification factor, the equivalent for this data set would be group 3-6. The measured contrast values are shown in Table 1. Because group 3-6 was affected by vignetting at position A, the vertical contrast values for the slightly higher frequency group 4-1 were substituted. These results are consistent with those found during final assembly.

3 Photometric calibration

Photometric calibration was accomplished by placing a double-opal diffuser in front of the instrument. When lighted up by a lamp shining down from the end of the tunnel, this arrangement provides an even and steady illumination pattern. Color filters were used to give a solar-like spectrum,

Table 1: Horizontal and vertical contrast values for bars 1.5 pixels wide, at various locations around the detector. The approximate pixel position for each group is also given.

Pixel Position	0°		120°		240°	
	H	V	H	V	H	V
(910,1480)	0.258	0.234	0.242	0.195	0.250	0.175
(1360,590)	0.332	0.315	0.339	0.324	0.342	0.326
(470,590)	0.313	0.261	0.292	0.273	0.268	0.263

and a photomultiplier tube was used for calibration purposes. The source brightness was measured at 0.14 foot-lamberts before pump-down, and 0.18 foot-lamberts after the chamber was reopened. We will use the average of 0.16 foot-lamberts in the analysis. Using the scaling factor of 0.563 foot-lamberts being equal to $10^{-9} B/B_\odot$, we can calculate that the calibration source is equal to 2.66×10^{-10} $B/B_\odot$. An 18% correction for in-band light raises this number to 3.14×10^{-10} $B/B_\odot$ (see Section 4).

The average signal was measured to be 157 DN at an exposure time of 60 seconds. Thus, a data rate of 1 DN/sec is equivalent to 1.20×10^{-10} $B/B_\odot$. Note that these numbers are based on the average signal at the detector. Because the internal polarizer only allows one state of polarization through, and thus cuts unpolarized light in half, the calibration parameter to be applied to B or pB values derived by rotating the polarizer is 6.0×10^{-11}.

4 Scattered light

To test scattered light, a very bright xenon arc lamp is sent down the tunnel. An aperture at the window where the light enters the tunnel defines the source size. The distance between this aperture and the COR1-A objective was 11 meters. The aperture size depends on the amount of defocus of this finite source at the occulter, combined with the chromatic aberration of the objective lens. Taking these considerations into account, the final aperture was sized at 76.5 mm. With this aperture, the solar brightness was measured to be 0.96 W/m^2 before pump-down, and 0.99 W/m^2 after the chamber was re-opened, with an average of 0.975 W/m^2. These measurements were made with bandpass filter #9 and the Gamma Scientific photometer in λ-mode at 656 nm. Given the measured characteristics of this filter, a solar brightness would be measured at 32.9592 W/m^2. Thus, we were exposing the instrument to $1/33.8^{th}$ of a solar brightness.

An earlier measurement of the lamp brightness, when a different aperture was installed in the tank, gave a brightness of 0.033 $B/B_\odot$ using the Gamma Scientific photometer with the bandpass filter, and 0.028 $B/B_\odot$ when using the same white-light photomultiplier used for the photometric calibration. From these data, we deduce that a correction of 18% needs to be applied to the photomultiplier data to take the specific COR1 wavelength bandpass into account. This factor was applied to the photometric calibration in Section 3.

Figure 4 shows the measured scattered light, multiplied by 33.8 to take the brightness of the lamp into account, and calibrated using the results from Section 3. The brightest spot in this image is 9.2×10^{-7} $B/B_\odot$. Based on their brightness and size, it is believed that the small ring-shaped features at various locations around the image are scattering sources on the front surface of the

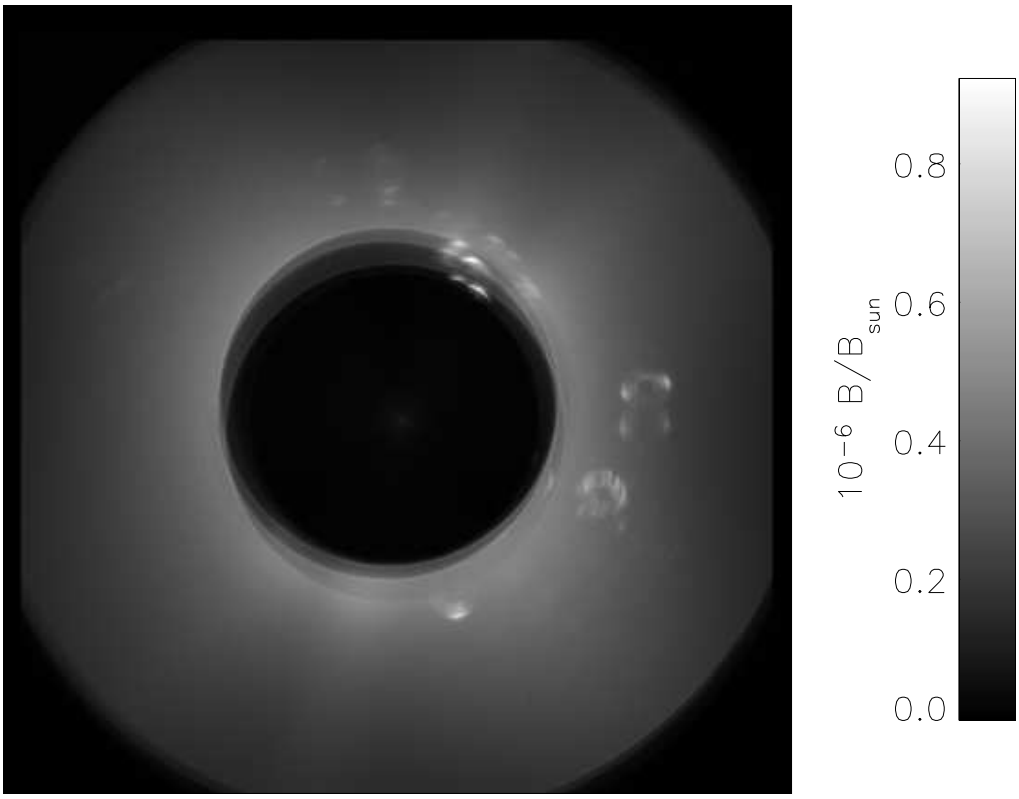

Figure 4: Scattered light image.

field lens. Figure 5 shows the average scatter as a function of radial distance from the center of the mask as determined in Section 5.

The data in Figure 4 were taken with an exposure time of 20 seconds. With a full solar flux, an exposure time of 0.6 seconds would give the same level of exposure. In fact, one should be able to go to twice this exposure time without saturating the detector.

There is a polarization signal to the scattered light pattern of ∼4%. However, it appears that this is because the light from the source is polarized by that amount, since the degree of polarization is fairly constant, and the phase angle is also relatively constant over the image. Induced polarization within the instrument should vary with azimuth.

5 Flat field

When the Xenon source used for the scattered light test is used with the door closed, it simulates the Sun shining on the door during flight. The resulting flat-field image is shown in Figure 6. The response is highly flat. There's a slight ∼3% contamination from scattered light extending outward from a central point in the middle of the mask shadow. This scattered light component shows up in a polarized brightness map, and has three dark spokes separated by 120°, which is probably related to one of the lens mounts. (The part of the polarized brightness component which matches the flat field is believed to be due to the intrinsic polarization of the source, since this was not seen in flat field images taken with a different source. See Section 4 for details about the polarization

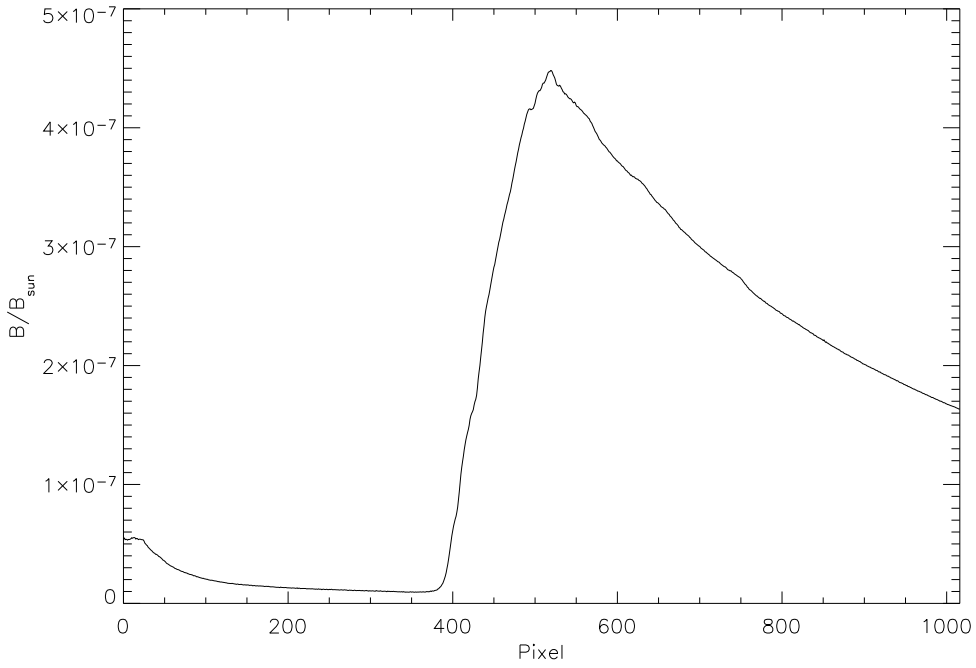

Figure 5: Average scattered light as a function of radial distance from the center of the focal plane mask.

of the source.)

The image in Figure 6 was taken with an exposure time of 10 seconds. Given that the source was $1/33.8^{th}$ of a solar brightness, an exposure of 0.3 seconds on orbit would give a similar exposure level on the detector, which is well within the capabilities of the instrument. In fact, one could go to almost double that exposure time before saturating the detector. The calibration window in the door is scheduled to be changed out for a flight window, but the difference in response is expected to be minor.

The inner and outer edges of the mask shadow are at radial distances of 397.5 and 513.2 pixels respectively. The center of the mask pattern is at pixel $i = 1065.91$, $j = 1026.36$.

6 Polarization response

To test the polarization response, a filter wheel was used to place a selection of polarizers in front of the double-opal used for the photometric calibration. One polarizer was oriented at 0°, and the other was oriented at -45°. In both cases, the results are consistent with 100% polarization within the noise. The polarizer offsets were measured to be $8\overset{\circ}{.}879 \pm 0\overset{\circ}{.}044$ and $11\overset{\circ}{.}323 \pm 0\overset{\circ}{.}145$ respectively. The small discrepency between these two numbers are probably due to alignment errors of the polarizers within the filter wheels. These results are consistent with the value of $11\overset{\circ}{.}04 \pm 0\overset{\circ}{.}28$ found during final assembly.

The signal during this test was extremely small, to the extent that the small changes in thermal signal during the observations became important, even when the temperature was controlled with

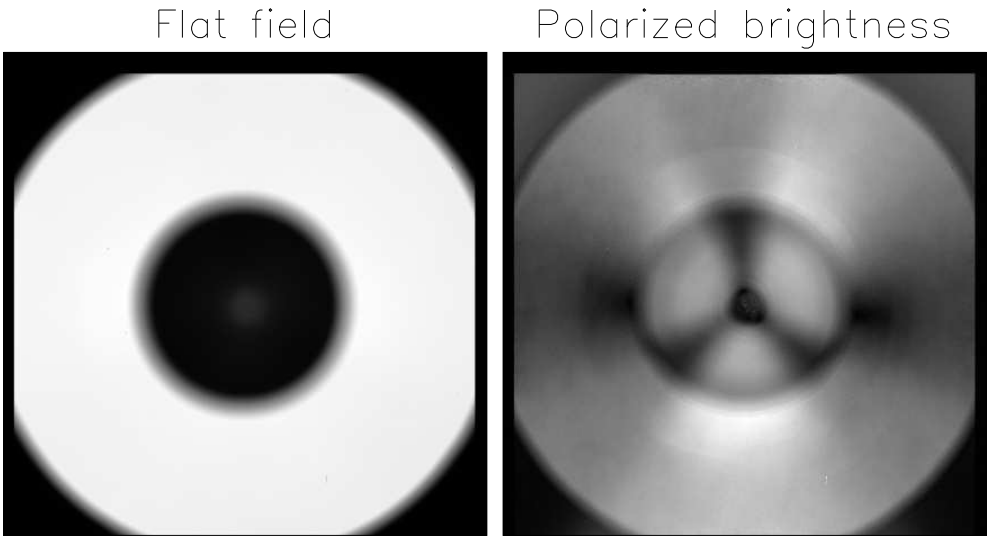

Figure 6: Flat field image, using the Xenon arc lamp shining on the calibration window in the COR1-A door. Also shown is a polarized brightness image of the scattered light associated with the flat field.

the CCD heater. In order to take this effect out, and to take out the effect of the anomalous software-induced 0.75 seconds extra exposure time compared to the dark images, the average signal in the four dark corners was subtracted from each image.

An additional filter wheel position held a circular polarizer. Unfortunately, the quarter-wave plate portion of this circular polarizer was tuned to a shorter wavelength than the COR1-A band-pass, so it was not a valid test of the system. For what it's worth, when observed with COR1-A, the light was seen to be $\sim$14% partially polarized at a phase angle of about -32° relative to the home position, or about -43° when the COR1-A offset angle is taken into account.

6.1 Partial polarization

A diffuser and two plates of glass, held at opposing 45° angles to the optical axis, were used to create partially polarized light in front of the instrument. The measured signal was polarized by $11.4\% \pm 0.5\%$, at a phase angle of $10\overset{\circ}{.}15 \pm 1\overset{\circ}{.}19$ relative to the home position. (When the COR1-A offset angle is taken into account, this is consistent with an angle of 0.) The variation over the field of view appears to be dominated by the scattered light pattern shown in Figure 6.

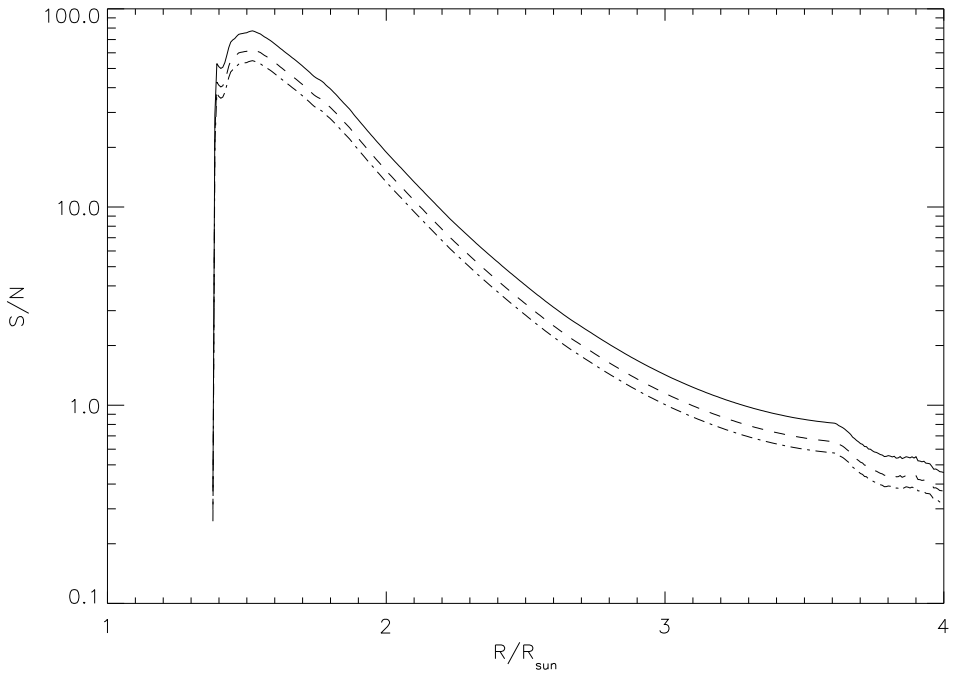

Figure 7: Average signal-to-noise ratio as a function of radial distance from the center of the focal plane mask for exposure times of 2 seconds (solid), 1.3 seconds (dashed), and 1 second (dash-dot).

6.2 Signal-to-noise ratio

To calculate the expected signal-to-noise ratio, the first step is to model the expected pB signal from the corona. This was modeled using the formula

$$\log_{10}(pB) = -2.66 - 3.55r + 0.460r^2 \tag{1}$$

where r is the distance in solar radians. The modeled k-corona polarized brightness thus ranges from 2×10^{-7} $B/B_\odot$ at the inner edge of the field of view to 3×10^{-10} $B/B_\odot$ at the outer edge. The flat field of Figure 6 is applied to this brightness distribution, which is then combined with the scattered light pattern of Figure 4. Assuming that the CCD is digitized at 15 e^-/DN, and that the pixels are binned 2×2, one can calculate the ratio between the signal and the Poisson noise. The average signal-to-noise ratio is shown in Figure 7 for an exposure time of 2 seconds, where some of the small bright features may saturate, at 1.3 seconds, where all of the features should be below saturation, and at 1 second, which is the design goal. The S/N peaks at around 50–75 near 1.5 $R/R_\odot$, depending on the exposure time, and drops to unity at around 3.0–3.3 $R/R_\odot$. There are small drops in S/N associated with the discrete scattered light features in Figure 4, on the order of 30–50%.

7 Exposure time test

The linearity of the instrumental exposure time had been tested during final assembly, but thermal effects caused it to saturate at the highest exposure times. Running the instrument cold allowed

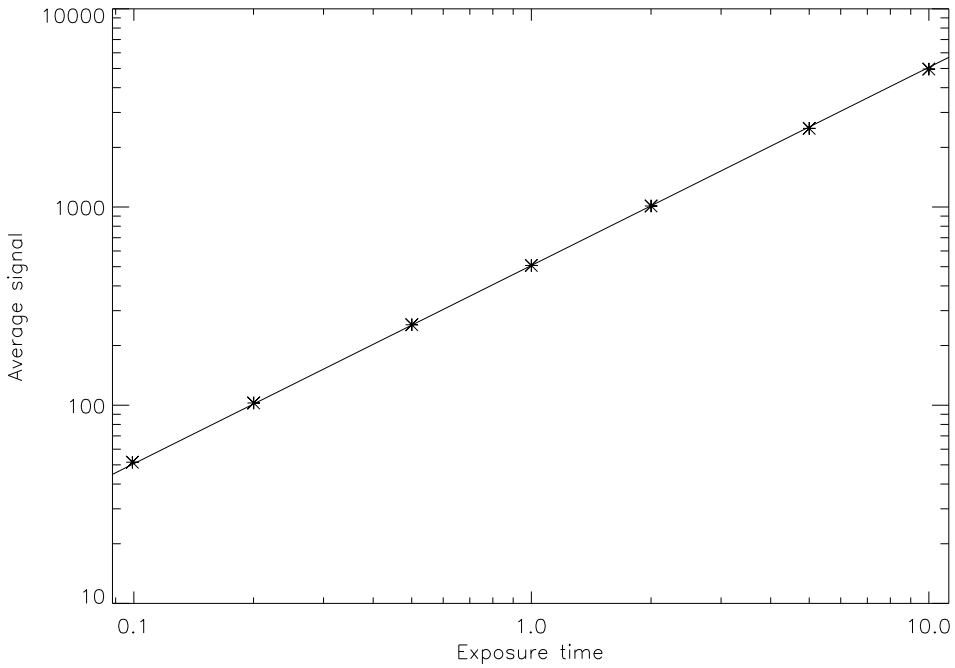

Figure 8: Comparison between measured signal and exposure time.

this test to be carried out at greater accuracy. The result is shown in Figure 8

8 Conclusions

The COR1-A instrument meets all of its performance goals for scattered light, resolution, sensitivity, and polarization response.

Acknowledgments

These measurements would not have been possible without a lot of work from a large number of people. I would particularly like to thank Sam Hetherington, Mike Pilecki, Les Putnam, Christian Keyser, Randy Waymire, Greg Wyotko, Therese Errigo, and Dave Clark.